ApJ submitted, Sept. 14, 2012
Preprint typeset using LaTeX style emulateapj v. 5/2/11

arXiv:1209.3325v1 [astro-ph.HE] 14 Sep 2012

A FAST FLARE AND DIRECT REDSHIFT CONSTRAINT IN FAR-ULTRAVIOLET SPECTRA OF THE BLAZAR S5 0716+714

Charles W. Danforth, Krzysztof Nalewajko, Kevin France, & Brian A. Keeney
CASA, Department of Astrophysical & Planetary Sciences, University of Colorado, 389-UCB, Boulder, CO 80309;
danforth@casa.colorado.edu

ApJ submitted, Sept. 14, 2012

ABSTRACT

The BL Lacertae object S5 0716+714 is one of the most studied blazars on the sky due to its active variability and brightness in many bands, including VHE gamma rays. We present here two serendipitous results from recent far-ultraviolet spectroscopic observations by the Cosmic Origins Spectrograph onboard the *Hubble Space Telescope*. First, the blazar increased in flux rapidly by $\sim 40\%$ (-0.45 mag h^{-1}) followed by a slower decline ($+0.36$ mag h^{-1}) to previous far-UV flux levels during the course of our 7.3 hour HST observations. We model this flare using asymetric flare templates and constrain the physical size, and energetics of the emitting region. Furthermore, the spectral index of the object softens considerably during the course of the flare from $\alpha_\nu \approx -1.0$ to $\alpha_\nu \approx -1.4$. Second, we constrain the source redshift directly using the > 30 intervening absorption systems. A system at $z = 0.2315$ is detected in Lyα, Lyβ, O VI, N V, and C III and defines the lower bound on the source redshift. No absorbers are seen in the remaining spectral coverage ($0.2315 < z_{Ly\alpha} \lesssim 0.47$) and we set a statistical upper bound of $z < 0.304$ (90% confidence) on the blazar. This is the first direct redshift limit for this object and is consistent with literature estimates of $z = 0.31 \pm 0.08$ based on the detection of a host galaxy.

Subject headings: BL Lacertae objects: individual: S5 0716+714, radiation mechanisms: nonthermal, galaxies: jets, galaxies: active, intergalactic medium, quasars: absorption lines, ultraviolet: general

1. INTRODUCTION

Blazars are a class of AGN in which non-thermal continuum emission is relativistically beamed into our line of sight, rendering them extremely bright across many wavebands at cosmological distances. S5 0716+714 is one of the most extensively studied blazars in the sky. It belongs to the blazar sub-class of BL Lacertae Objects (BL Lacs) which are known for their smooth non-thermal continua without clear emission lines. This lack of identifying spectral features makes the source redshifts, and hence the physical characteristics of these astrophysically interesting objects, very challenging to determine unambiguously.

Spectroscopically, S5 0716+714 was first studied in the optical band by Biermann et al. (1981) who found a completely featureless spectrum. No emission or absorption lines were ever identified in this source, despite several attempts (Stickel et al. 1993; Vermeulen & Taylor 1995; Rector & Stocke 2001; Finke et al. 2008). Nilsson et al. (2008) detected an excess in the point spread function of S5 0716+714 which is consistent with a host galaxy at $z = 0.31 \pm 0.08$. This range is consistent with the Stickel et al. (1993) identification of a pair of galaxies near the sight line at $z \simeq 0.26$, suggesting that the host is part of a galaxy group. Detection of S5 0716+714 in Very-High-Energy (VHE) gamma-rays by the MAGIC telescope led to different upper limits on the source redshift: $z \lesssim 0.5$ (Anderhub et al. 2009), and $z < 0.21 \pm 0.09$ (Prandini et al. 2010), though these depend on the poorly-characterized cosmic infrared background.

Blazars are also known for variability. Even amongst blazars, S5 0716+714 is well known for its strong and persistent optical variability with a duty cycle of $\sim$ 90% (Ostorero et al. 2006). Intraday variability (IDV) is routinely measured in this source with the reported maximum variability rates of $\sim 0.1 - 0.16$ magnitudes per hour (Wagner et al. 1996; Wu et al. 2005; Villata et al. 2000; Montagni et al. 2006; Ostorero et al. 2006; Nesci et al. 2002) to as high as 0.38 magnitudes per hour (Chandra et al. 2011). An extensive statistical analysis by Montagni et al. (2006) showed that variability rates of order $\sim 0.1\,\mathrm{mag\,hr^{-1}}$ usually last for no more than two hours, and their duty cycle is only a few percent. Asymmetric flares, with the increase rate on average faster than the decline rate, were found by Wagner et al. (1996) and Nesci et al. (2002), see, however, Ghisellini et al. (1997) and Montagni et al. (2006). Quasi-periodic oscillations were claimed over short time intervals with various periods: $\sim$ 1 day and $\sim$ 7 days (Quirrenbach et al. 1991; Wagner et al. 1996), $\sim$ 4 days (Heidt & Wagner 1996), and even as fast as $\sim$ 15 minutes (Rani et al. 2010).

BL Lac objects are extremely useful as probes of intervening material. High signal-to-noise (S/N) optical and ultraviolet spectral observations are possible if the blazar is observed during a bright state. Their smooth, power-law continua make it possible to distinguish weak, broad intergalactic absorption features from weak features in the background source continuum. It was for this reason that S5 0716+714 was observed by the Cosmic Origin Spectrograph on the *Hubble Space Telescope* (HST/COS; Green et al. 2012).

The far-ultraviolet (FUV) spectrum of S5 0716+714 provides an excellent dataset relevant to IGM cosmology

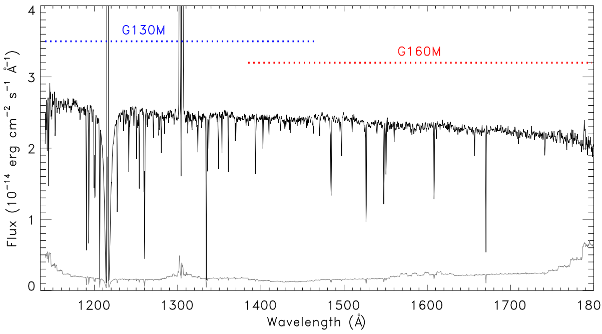

Fig. 1.— Coadded COS spectrum of S5 0716+714. Flux has been scaled to the first exposure (however, see discussion in Section 3.1) and smoothed by 35 pixels (approximately five resolution elements). Shaded data shows coadded photon noise. Sharp emission features are geocoronal airglow. The spectral ranges of the two medium-resolution, far-UV gratings on COS are shown.

which will be presented as part of a much larger study of the low-redshift IGM (Danforth et al. 2013, in prep). We present here two serendipitous discoveries from the S5 0716+714 observations. First, our five-orbit HST observations happened to observe a fast, asymmetric flare during which the blazar brightened by $> 35\%$ and then faded to approximately the flux level at the start of our observations. We discuss the flare and changes to the spectral energy distribution (SED) in Section 3. Second, in Section 4, we use the observed intervening absorption systems (the Lyα forest) along the sight line to place the first direct constraints on the source redshift of S5 0716+714. We discuss and summarize our results in Section 5.

2. OBSERVATIONS AND TIMING ANALYSIS

S5 0716+714 was observed with the Cosmic Origins Spectrograph (COS) on December 27, 2011, as part of HST program 12025 (PI: Green). Two exposures were made during each of five HST orbits over the course of 7.3 hours; the first five exposures with the G130M ($1135 < \lambda < 1450$ Å, 6.00 ksec) grating, the second five with the G160M ($1400 < \lambda < 1795$ Å, 8.25 ksec) gratings. The ten exposures were obtained from the Mikulski Archive for Space Telescopes (MAST) and reprocessed with a recent version of CALCOS (2.17.3a). The calibrated, one-dimensional spectra were next coadded with the custom IDL procedures described in detail by Danforth et al. (2010). We present the coadded COS spectrum of S5 0716+714 in Figure 1 (however, see the cautions regarding coaddition of a strongly varying source in Section 3.1.)

A Voigt profile fit to the Galactic Lyα profile in the G130M data gives a column density of $\log N(HI) = 20.372 \pm 0.003$. This corresponds to a color excess of $E(B-V) = 0.045$ and we deredden all observed fluxes via Fitzpatrick (1999)[1].

Many AGN show some degree of variability between one epoch and another and our coaddition software automatically scales exposures from different epochs to correct this (usually minor) effect. However, during coaddition of the S5 0716+714 data, it was noticed that the mean flux varied by as much as 35% during the course of 7.3 hours. COS is a photon-counting instrument; the arrival time of each photon is recorded as well as the two-dimensional position on the detector. It is therefore possible to extract very high resolution (~ 30 ms) time-domain data (France et al. 2010). We extract an $[x_i,y_i,t_i]$ photon list from each exposure i and coadd these to create a master $[x,y,t]$ photon list. The total number of counts in a $[\Delta x,\Delta y]$ box is integrated over a timestep Δt. We use a timestep of $\Delta t = 120$ s for S5 0716+714 to balance time-resolution with reasonable photometric precision. Continuum count rates are extracted over ~ 30 (37) Å integration regions for the G130M (G160M) grating at four nominal far-UV wavelengths ($1190 = [1178.6 - 1208.5$ Å] and $1390 = [1377.8 - 1407.7$ Å] in G130M; $1460 = [1447.9 - 1484.6$ Å] and $1520 = [1507.3 - 1544.0$ Å] in G160M). Narrow interstellar and intergalactic absorption lines are present in the data (see Figure 1), however these features only remove a small number of photons relative to the bright continuum emission on 30 Å scales, therefore ignoring narrow absorbers does not significantly impact the photometry produced here. The instrumental background is computed in a similar manner, with extraction boxes offset below the active science region of the detector. The instrumental background contributes $< 0.6\%$ of the total photons measured in each extraction region.

So that photometry from the blue G130M and red G160M gratings can be compared, flux-callibrated spectra for each exposure ($\sim 20 - 28$ min) are fitted with a power law of the form $f(\lambda) = f(\lambda_0) \times (\lambda/\lambda_0)^{\alpha_\lambda}$ normalized at $\lambda_0 = 1400$ Å, a wavelength covered by both gratings. Raw light curves in units of counts s^{-1} are extracted in the wavelengths intervals defined above and in 2-min time intervals. Flux calibrated light curves at λ_0 are obtained by dividing the raw light curves by exposure-averaged count rates in the same wavelengths intervals, and by multiplying them by $f(\lambda_0)$. The result is a nearly-continuous, flux-calibrated light curve for S5 0716+714 (Figure 2) at 1400 Å, interupted only by four periods of Earth occultation. Henceforth, all times are quoted in hours starting from MJD 55922 (0:00 UT on December 27, 2011).

3. A FAST FLARE IN THE FAR-ULTRAVIOLET

Figure 2 shows the strong source variability during our five-orbit (7.3 h) HST observing period; the blazar brightened by a factor of $\sim 40\%$ (0.36 mag) before fading to very nearly the initial intensity. Most dramatically, the source showed a monotonic flux increase of 0.17 mag during 0.39 h, with the average variability rate of -0.45 mag h^{-1} during the second orbit. During the third orbit, we observed a quasi-monotonic flux decrease of $+0.11$ mag over 0.26 h, with an average variability rate of $+0.36$ mag h^{-1}.

Even though there are gaps in our light curve due to Earth occultation, the variability appears to be fairly simple. Hence, we model the light curve with a constant background flux level F_0 and a single flare template which is described by a function

$$f_i(t) = \frac{2\,F_i}{\exp\left(\frac{t_i - t}{T_{\rm r,i}}\right) + \exp\left(\frac{t - t_i}{T_{\rm d,i}}\right)} \qquad (1)$$

---

[1] Note that the absorption-derived color excess measured here is $\sim 50\%$ larger than the extinction value derived from the low-resolution Schlegel, Finkbiner, & Davis (1998) dust maps.

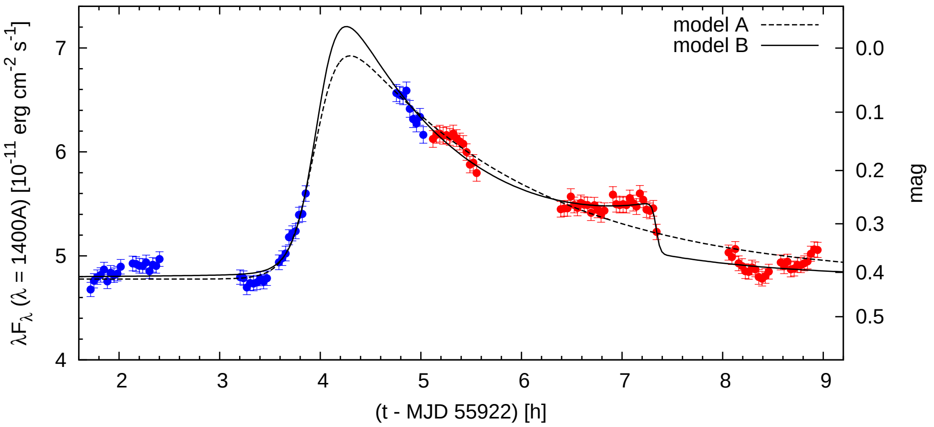

FIG. 2.— Far-UV light curve of S5 0716+714, presented as dereddened λF_λ values at $\lambda = 1400$Å extracted in 120 s time bins. Blue and red points show data collected using the G130M and G160M gratings, respectively. The overall light curve was fitted with two models consisting of one and two flare templates. The right axis shows magnitude calculated relative to the flux density level of 7×10^{-11} erg s^{-1} cm^{-2}.

TABLE 1
FLARE MODEL PARAMETERS[a]

Parameter	Model A	Model B
F_0	4.78 ± 0.03	4.79 ± 0.02
F_1	1.37 ± 0.07	1.59 ± 0.12
t_1	3.97 ± 0.05	3.99 ± 0.05
$T_{r,1}$	0.13 ± 0.04	0.12 ± 0.03
$T_{d,1}$	1.85 ± 0.12	1.28 ± 0.12
F_2	···	0.25 ± 0.04
t_2	···	7.34 ± 0.02
$T_{r,2}$	···	1.40 ± 0.53
$T_{d,2}$	···	0.02 ± 0.02
$\bar{\chi}^2$	5.1	3.2

[a] Flux density in 10^{-11} erg cm^{-2} s^{-1} and times in hours. Peak times are in hours since MJD 55922.

with four parameters: flare normalization F_i, flux raising time scale $T_{\rm r,i}$, flux decay time scale $T_{\rm d,i}$, and epoch t_i corresponding roughly to the flare maximum (Abdo et al. 2010). This Model A is shown in Figure 2, and its parameters are reported in Table 1. The fit quality is mediocre ($\bar{\chi}^2 = 5.1$) and the largest residuals are observed during the late stage of the flare. Hence, we consider a more detailed Model B, which includes a second flare template. This model provides a substantial improvement in the fit quality ($\bar{\chi}^2 = 3.2$), and the remaining residuals do not show any long-term structure. The main difference in the main flare parameters in Model B, compared to Model A, are higher flare amplitude F_1 and shorter flux decay time scale $T_{\rm d,1}$. The background flux level F_0, flux raising time scale $T_{\rm r,1}$, and the moment of peak flux t_1 are consistent between models A and B. The second flare template $f_2(t)$ of Model B has poorly constrained characteristic time scales; in particular, the very fast decay time $T_{\rm d,2}$ is almost entirely determined by the final 120 s bin at the end of the fourth orbit. In Section 5, we discuss the physical implications of the main flare parameters.

3.1. *Spectral Energy Distribution*

Broad spectral coverage allows us to monitor any changes in the spectral index of S5 0716+714. Though the spectral "throw" of any individual observation is relatively small ($\Delta\lambda/\lambda \sim 23\%$), they show significantly different spectral indices during the course of the HST observations. We convert our measured α_λ values (Section 2) to the more conventional α_ν via the relationship $\alpha_\nu = -(2 + \alpha_\lambda)$ (Shull, Stevans & Danforth 2012). The SED softens monatonically at the rate of $\Delta\alpha_\nu \approx -0.05$ h^{-1} from $\alpha_\nu \approx -1.0$ at the beginning of the observation to $\alpha_\nu \approx -1.2$ near the flare maximum to $\alpha_\nu \approx -1.4$ at the end of the observation as shown in Fig. 3. This trend is consistent with measured flux ratios from the blue and red ends of each spectral range.

Plotting spectral index versus intensity (right panel of Fig. 3) gives what could be interpretted as a clockwise hysteresis loop although α_ν decreases monatonically throughout our observation and the loop does not close. Kirk, Rieger, & Mastichiadis (1998) model electron acceleration in relativistic shocks and see that the directionality of the loop can be related to the propagation of a flare through the SED of the blazar. A clockwise loop in α_ν-flux space is typical for blazars observed at energies lower than their synchrotron peak. S5 0716+714 is a high-peaked BL Lac (HBL) object peaking in the X-rays,

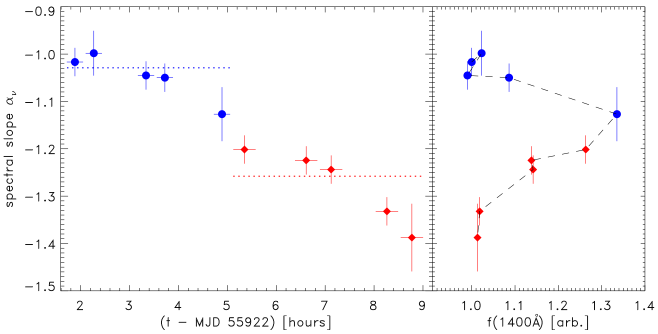

FIG. 3.— Power law fits to the individual COS observations show a softening of the SED (decreasing α_ν) throughout the HST observation (left panel). Blue circles show fits to the G130M ($1140 < \lambda < 1450$ Å) exposures while red diamonds denote G160M ($1400 < \lambda < 1795$ Å) exposures. Dotted blue and red lines show the fitted index for coadded G130M and G160M exposures. The spectral index versus extrapolated flux at 1400 Å (right panel) suggests a clockwise hysteresis loop.

so this is the expected behavior as synchrotron heating or cooling information propagates from higher to lower energies through the SED. However this is in the opposite sence to the loop seen in the optical observations of (Carini, Walters, & Hopper 2011).

The highest-quality spectra can often be obtained by scaling the individual exposures and coadding them onto a common wavelength scale. However, the significant change in the spectral index of S5 0716+714 during the observations makes any SED derived from the combined observations suspect. Combining just the observations in the same far-UV waveband produce slopes of $\alpha_\nu \approx -1.03$ and -1.26 for G130M and G160M channel coadditions, respectively (dotted horizontal lines in Figure 3). Both slope values are typical of those of the individual observations, but we caution against trying to determine an overall SED from the combined far-UV observations.

4. REDSHIFT OF S5 0716+714

Determining the source redshift of featureless AGN can be difficult, especially at higher redshift where the host galaxy cannot be easily identified. Redshift limits can be inferred through indirect means (host galaxy non-detection, gamma ray emission, etc.). A direct lower limit to the source redshift can be determined through intermediate absorption lines in moderate-resolution data (usually in the UV). An automated line-finding algorithm (Danforth et al. 2013, in prep) finds ~ 37 intervening Lyα absorption systems detected to greater than 4σ significance in the COS spectrum of S5 0716+714. Figure 4 shows the observed COS spectral range with measured Lyα systems along the top edge in both wavelength and redshift space. The reddest of these lines is at 1497 Å, corresponding to $z_{\rm abs} = 0.2315$, is confirmed by corresponding detections in higher-order Lyman lines (Lyβ, Lyγ) as well as metal ions (O VI, N V) thus setting a firm lower limit on the redshift of S5 0716+714. The remaining spectral range (1497Å $< \lambda <$ 1795Å; $0.232 < z_{Ly\alpha} < 0.47$) is devoid of Ly$\alpha$ absorption to a 4σ limiting equivalent width of ~ 30 mÅ (log $N_{\rm HI} \sim 12.7$). This technique was first used in Danforth et al. (2010) to constrain the upper redshift limit of 1ES 1553+113 and we refine the methodology here.

We calculate the expected density of intervening Lyα systems per unit redshift, $d\mathcal{N}(z)/dz$ (shaded curve in Figure 4). The minimum column density absorber that can be detected at a 4σ level is predicted based on the S/N in the data (Keeney et al. 2012) and the $d\mathcal{N}/dz$ at that limiting column is drawn from the large, low-redshift IGM surveys of Danforth & Shull (2008) and Tilton et al. (2012). We assume no evolution in the Lyα forest over this small redshift, but including a modest evolution produces negligible changes in the predicted absorber distribution. The overall density of absorbers toward S5 0716+714 (black data points) follows the predicted curve consistently though with variations in individual redshift bins most likely due to cosmic variance.

To constrain the upper limit on source redshift, we truncate the predicted $d\mathcal{N}/dz$ curve at a range of redshifts and compare the modeled absorber distribution to the observed distribution using a K-S test. S5 0716+714 can be constrained to $0.2315 < z \lesssim 0.2668$ (68% confidence), $0.2315 < z \lesssim 0.3035$ (95%), or $0.2315 < z \lesssim 0.3407$ (99%).

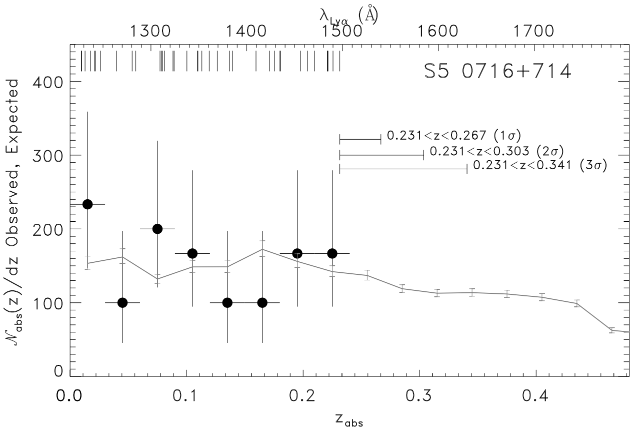

FIG. 4.— Intervening absorption lines provide the source redshift of S5 0716+714. Vertical ticks at the top of the figure show the wavelength/redshift location of all ~ 37 intervening Lyα systems seen towards the blazar. The line density as a function of redshift, $d\mathcal{N}(z)/dz$ is shown in bins of $dz = 0.03$ and compared with the expected line density (gray) based on the quality of the COS data and the distribution of absorbers at low-redshift in a statistical sample (Danforth & Shull 2008; Tilton et al. 2012). We truncate the statistical sample at different redshifts and compare to the observed distribution with a K-S test. The upper limit is constrained to $z < 0.304$ ($z < 0.341$) to a 2σ (3σ confidence limit). The strong absorption system at $z = 0.2315$ defines the lower redshift limit.

Weak Lyα emission is occasionally seen from BL Lac objects (Stocke, Danforth, & Perlman et al. 2011) and is an unambiguous, direct way of determining the redshift of blazars to high precision. The only deviations from a smooth power-law continuum seen in the coadded G160M data are likely artifacts produced by the coadding individual exposures with rapidly changing spectral index and none is convincing as Lyα emission at $z > 0.2315$. We set a 3σ upper limit of $I({\rm Ly}\alpha) \lesssim 5 \times 10^{-15}$ erg cm^{-2} s^{-1} ($EW \lesssim 115$ mÅ) by measuring the equivalent width detection limit (Keeney et al. 2012) for an emission feature with FWHM$\approx$ 3 Å in the rest frame (typical of those seen by Stocke et al. in Mrk 421, PKS 2005−489 and Mrk 501). This intensity limit translates to an isotropic luminosity of $L({\rm Ly}\alpha) \lesssim 6.5 \times 10^{41}$ erg s^{-1}. This upper limit is several times greater the Lyα luminosity observed in lower-redshift BL Lacs, so it is not surprising that no emission is seen in S5 0716+714.

5. DISCUSSION

We performed the deepest and most precise far-UV spectroscopic observation of S5 0716+714 to date. We did not identify any emission lines, and thus the source redshift remains unknown. However, the detection of narrow Lyα forest features enables the deermination of a new, independent constraint — $0.2315 < z < 0.304$ at the 2σ confidence level. This redshift range is consistent with the result of Nilsson et al. (2008), $z = 0.31 \pm 0.08$, based on the photometric detection of the host galaxy as well as the intriguing possibility that S5 0716+714 is associated with a group of nearby galaxies observed at redshift $z = 0.26$ (Stickel et al. 1993). We note that the uncertainty in our estimate is based on the statistical properties of the low-redshift Lyα forest along many sight lines, while the uncertainty of the Nilsson et al. (2008) estimate is based on the statistics of the host galaxy luminosities for BL Lacs. Our source redshift estimate is also consistent with the crude upper limit $z < 0.21 \pm 0.09$ obtained by Prandini et al. (2010) from modeling the source spectral energy distribution at VHE gamma-rays and also with the $z \lesssim 0.5$ estimate of (Anderhub et al. 2009).

Our observations of S5 0716+714 coincided with a period of rapid flux variability. This is not surprising, since this source is well known for almost uninterrupted variability at multiple time scales. We detected episodes of very fast variability rate, up to 0.45 mag h^{-1}. This higher than the maximum observed variability rate found in the most extensive study of IDV in this source (Montagni et al. 2006), but comparable to the variability rate found by Chandra et al. (2011) during one night out of five. It seems that such fast variability rates are limited to the periods of a fraction of hour. This appears to be consistent with the general trend that faster variability rates last for shorter time intervals (see Figure 7 in Montagni et al. 2006). It is also known that the frequency of light curve segments with constant variability rate decreases exponentially with increasing variability rate. This would indicate rapid flares such as the one we observed with HST/COS, while spectacular, are probably not important in the overall source energetics. However, the study of Montagni et al. (2006) uses much longer sampling rates, and to obtain a statistical picture of intra-hour variability of this blazar one needs a much larger sample of high-cadence observations.

The decomposition of the observed light curve of S5 0716+714 into a coherent flaring component and a quasi-static background (Model B, above) allows us to constrain the physics of the emitting region producing the flare. The flux raising time scale of the flaring component, $T_{\rm r,1} = (7.4 \pm 1.8)$ min, indicates the emitting region radius

$$R \lesssim \mathcal{D} c T_{\rm r,1}/(1+z) \simeq 3.4 \times 10^{-5} (\mathcal{D}/10)\ {\rm pc} \qquad (2)$$

(for $z = 0.26$), where $\mathcal{D}$ is the Doppler factor of the emitting region. The flux decay time constrains the cooling time scale

$$T_{\rm d,1} \gtrsim t_{\rm cool,obs} = \frac{3(1+z) m_{\rm e} c}{4 \mathcal{D} \sigma_{\rm T} u_0' \gamma_{\rm e}}, \qquad (3)$$

where $u_0' = u_B' + u_{\rm rad}' = (1+q) B'^2/(8\pi)$ is the co-moving energy density of the magnetic field (determining the synchrotron cooling rate) plus the diffuse radiation (determining the inverse-Compton cooling rate), $q \simeq L_{\rm IC}/L_{\rm syn}$ is the Compton dominance parameter (which for BL Lacs is of order of unity), and $\gamma_{\rm e}$ is the characteristic random Lorentz factor of electrons producing the observed FUV emission. Since the FUV continuum emission is produced by the synchrotron process, we can use the expression for the observed frequency of the synchrotron radiation,

$$\nu_{\rm syn,obs} = \frac{0.274\, \mathcal{D} e \gamma_e^2 B'}{(1+z) m_{\rm e} c} \simeq \frac{c}{1400\ \text{Å}}, \qquad (4)$$

to eliminate $\gamma_{\rm e}$ and obtain an estimate of the magnetic field strength in the emitting region

$$B' \gtrsim 2\ {\rm G} \times (\mathcal{D}/10)^{-1/3} (1+q)^{-2/3}. \qquad (5)$$

It follows that

$$\gamma_{\rm e} \lesssim 5300 \times (\mathcal{D}/10)^{-1/3} (1+q)^{1/3}. \qquad (6)$$

The apparent flare luminosity is

$$L_1 = 4\pi d_{\rm L}^2 F_1 \simeq 3.2 \times 10^{45}\ {\rm erg\, s^{-1}}. \qquad (7)$$

We use it to estimate the co-moving energy density of the synchrotron radiation

$$\begin{aligned} u_{\rm syn}' &= L_1/(4\pi c \mathcal{D}^4 R^2) \qquad (8) \\ &\gtrsim 78\ {\rm erg\, cm^{-3}} \times (\mathcal{D}/10)^{-6}. \end{aligned}$$

In a typical BL Lac, one can neglect the external radiation, and thus the total energy density of the diffuse radiation is $u_{\rm rad}' \simeq u_{\rm syn}'$. Using the estimate for B', we can write a direct relation between the Compton dominance parameter and the Doppler factor:

$$q/(1+q)^{4/3} \simeq 485 (\mathcal{D}/10)^{-16/3}. \qquad (9)$$

We can further use the apparent flare luminosity to estimate the number of electrons contributing to the FUV emission

$$\begin{aligned} N_{\rm e} &\simeq 6\pi L_1/(\sigma_{\rm T} c \mathcal{D}^4 B'^2 \gamma_{\rm e}^2) \qquad (10) \\ &\simeq 2.7 \times 10^{48} \times (\mathcal{D}/10)^{-8/3} (1+q)^{2/3}, \end{aligned}$$

and their co-moving energy density

$$\begin{aligned} u_{\rm e}' &\simeq 3 N_{\rm e} \gamma_{\rm e} m_{\rm e} c^2/(4\pi R^3) \qquad (11) \\ &\simeq 2400\ {\rm erg\, cm^{-3}} \times (\mathcal{D}/10)^{-6} (1+q). \end{aligned}$$

If we assume equipartition between electrons and the magnetic field, $u_{\rm e}' \simeq u_B'$ (Böttcher et al. 2009), we will obtain a very large Doppler factor, $\mathcal{D} \simeq 62$, and a very small Compton dominance parameter $q \simeq 0.031$. Such a scenario poses a severe problem of explaining the extremely efficient acceleration of the emitting region, but it predicts a negligible gamma-ray signature of the FUV flare via the Synchrotron Self-Compton (SSC) mechanism. If we instead assume that $q = 1$, we will still require a large Doppler factor, $\mathcal{D} \simeq 38$, but also a strong departure from the equipartition, with $u_{\rm e}'/u_{\rm B}' \simeq 62$. It should be noted that gamma-ray emission was detected in S5 0716+714 by MAGIC (Anderhub et al. 2009), AGILE (Vittorini et al. 2009) and *Fermi* at the level of $L_\gamma \sim (0.5-5) \times 10^{46}\ {\rm erg\, s^{-1}}$. Hence, the Compton dominance parameter q cannot be much larger than unity and some extreme physical parameter of the emitting region producing the fast FUV flare is unavoidable. This makes our case of a fast FUV flare similar to the fast gamma-ray flares observed in other BL Lacs (PKS 2155−304, Aharonian et al. 2007; Mrk 501, Albert et al. 2007) and one FSRQ (PKS 1222+216, Aleksić et al. 2011). They also seem to require extremely high Doppler factors (Begelman et al. 2008), and a number of theoretical scenarios were proposed to explain them (Levinson 2007; Stern & Poutanen 2008; Ghisellini & Tavecchio 2008; Giannios et al. 2009; Lyutikov & Lister 2010; Nalewajko et al. 2011). In the case of S5 0716+714, we cannot constrain the distance of the emitting region from the central black hole, and thus we have greater freedom of theoretical scenarios than in the case of PKS 1222+216 (Tavecchio et al. 2011; Nalewajko et al. 2012).

We observed strong spectral variability with the systematic spectral index change of $\Delta\alpha_\nu = -0.4$ over the course of ~ 7 h. A diagram of spectral index vs. flux density shows probable clockwise hysteresis. Strong intraday spectral variations in the optical/UV band is rarely reported. For example, Wu et al. (2012) found the $B-R$ color to vary with the amplitude of $|\Delta(B-R)| \simeq 0.08$ within an hour. This corresponds to $|\Delta\alpha_\nu| = |\Delta(B-R)|/0.413 \simeq 0.2$, which means a significantly faster variability rate. However, we have found no case of a systematic spectral index variation over several hours.

Spectroscopic observations of blazars are proving to be versatile tool with which to study a range of astrophysical processes from galactic structure to cosmology to the study of AGN processes. Our observations of S5 0716+714 illustrate the power of time-domain sensitivity as well. Not only is the Cosmic Origins Spectrograph the most sensitive far-UV spectroscopic instrument ever flown, but the temporal resolution can be exploited to look for microvariability on very short time scales. A number of other blazars have been observed with HST/COS as part of a larger program on low-redshift cosmology. Many cover only a short time period (1-3 HST orbits), but those with similar 5-orbit observations do not show appreciable variability. We will continue to both look for notable variability in AGN observations and to determine the source redshifts of poorly-constrained blazars through spectroscopy of their intervening absorbers.

The authors wish to acknowledge fruitful discussions with John Stocke. This work was supported by NASA grants NNX08AC146 and NAS5-98043 to the University of Colorado at Boulder. The authors made extensive use of the MAST, ADS, and IGwAD Archives during this work.

Facility: HST (COS)

REFERENCES

Abdo, A. A., Ackermann, M., Ajello, M., et al. 2010, ApJ, 722, 520
Aharonian, F., et al., 2007, ApJ, 664, L71
Albert, J., et al., 2007, ApJ, 669, 862
Aleksić, J., et al., 2011, ApJ, 730, L8
Anderhub, H., Antonelli, L. A., Antoranz, P., et al. 2009, ApJ, 704, L129
Begelman, M. C., Fabian, A. C., Rees, M. J., 2008, MNRAS, 384, L19
Biermann, P., Duerbeck, H., Eckart, A., et al. 1981, ApJ, 247, L53
Böttcher, M., Reimer, A., & Marscher, A. P., 2009, ApJ, 703, 1168
Carini, M. T., Walters, R., & Hopper, L., 2011, AJ, 141, 49
Chandra, S., Baliyan, K. S., Ganesh, S., & Joshi, U. C. 2011, ApJ, 731, 118
Danforth, C. W., Keeney, B. A., Stocke, J. T., Shull, J. M., & Yao, Y. 2010, ApJ, 720, 976
Danforth, C. W., & Shull, J. M. 2008, ApJ, 679, 194
Finke, J. D., Shields, J. C., Böttcher, M., & Basu, S. 2008, A&A, 477, 513
Fitzpatrick, E. L. 1999, PASP, 111, 63
France et al. 2010, ApJ, 715, 596
Ghisellini, G., Villata, M., Raiteri, C. M., et al. 1997, A&A, 327, 61
Ghisellini, G., & Tavecchio, F., 2008, MNRAS, 386, L28
Giannios, D., Uzdensky, D. A., & Begelman, M. C., 2009, MNRAS, 395, L29
Green, J. C., Froning, C. S., Osterman, S., et al. 2012, ApJ, 744, 60
Heidt, J., & Wagner, S. J. 1996, A&A, 305, 42
Keeney, B. A., Danforth, C. W., Stocke, J. T., France, K., & Green, J. C. 2012, PASP submitted (ArXiv 1206.2951)
Kirk, J. G., Rieger, F. M., & Matichiadis, A. 1998, A&A, 333, 452
Levinson, A., 2007, ApJ, 671, L29
Lyutikov, M., & Lister, M., 2010, ApJ, 722, 197
Montagni, F., Maselli, A., Massaro, E., et al. 2006, A&A, 451, 435
Nalewajko, K., Giannios, D., Begelman, M. C., Uzdensky, D. A., Sikora, M., 2011, MNRAS, 413, 333
Nalewajko, K., Begelman, M. C., Cerutti, B., Uzdensky, D. A., & Sikora, M. 2012, MNRAS, 425, 2519
Nesci, R., Massaro, E., & Montagni, F. 2002, PASA, 19, 143
Nilsson, K., Pursimo, T., Sillanpää, A., Takalo, L. O., & Lindfors, E. 2008, A&A, 487, L29
Ostorero, L., Wagner, S. J., Gracia, J., et al. 2006, A&A, 451, 797
Quirrenbach, A., Witzel, A., Wagner, S., et al. 1991, ApJ, 372, L71
Prandini, E., Bonnoli, G., Maraschi, L., Mariotti, M., & Tavecchio, F. 2010, MNRAS, 405, L76
Rani, B., Gupta, A. C., Joshi, U. C., Ganesh, S., & Wiita, P. J. 2010, ApJ, 719, L153
Rector, T. A., & Stocke, J. T., 2001, AJ, 122, 565
Sbarufatti, B., Treves, A., & Falomo, R. 2005, ApJ, 635, 173
Schlegel, D. J., Finkbeiner, D. P., & Davis, M., 1998, ApJ, 500, 525
Shull, J. M., Stevans, M, & Danforth, C. W. 2012, ApJ, 752:162
Stern, B. E., & Poutanen, J., 2008, MNRAS, 383, 1695
Stickel, M., Fried, J. W., & Kuehr, H. 1993, A&AS, 98, 393
Stocke, J. T., Danforth, C. W., & Perlman, E. S. 2011, ApJ, 732, 113
Tavecchio, F., Becerra-Gonzalez, J., Ghisellini, G., Stamerra, A., Bonnoli, G., Foschini, L., Maraschi, L., 2011, A&A, 534, A86
Tilton, E. M., Danforth, C. W., Shull, J. M., & Ross, T. L. 2012, ApJ, submitted (ArXiv 1204.3623)
Vermeulen, R. C., & Taylor, G. B. 1995, AJ, 109, 1983
Villata, M., Mattox, J. R., Massaro, E., et al. 2000, A&A, 363, 108
Vittorini, V., Tavani, M., Paggi, A., et al. 2009, ApJ, 706, 1433
Wagner, S. J., Witzel, A., Heidt, J., et al. 1996, AJ, 111, 2187
Wu, J., Peng, B., Zhou, X., et al. 2005, AJ, 129, 1818
Wu, J., Böttcher, M., Zhou, X., et al. 2012, AJ, 143, 108